Spring 2017

Synthesis of Copper Oxide Nanoparticles in Droplet Flow Reactors

Christopher Reilly
University of New Hampshire, Durham

Synthesis of Copper Oxide Nanoparticles in Droplet Flow Reactors

Abstract

Synthesis of metal oxide nanoparticles within droplet flow reactors is advantageous over batch synthesis due to the elimination of concentration and temperature gradients inside the reactor and prevention of reactor fouling. We present results on the synthesis of copper oxide nanoparticles using aqueous droplets of copper acetate and acetic acid inside a bulk stream of sodium hydroxide in 1-octanol. Varying the copper acetate, acetic acid, and sodium hydroxide concentration resulted in needle-like and plate-like nanoparticles of varying sizes. The rate of mass transfer from the bulk to the droplet phase was found to increase with flow rate and addition of surfactants.

Keywords

CuO, Interphase synthesis, Two-phase, Flow reactor

Subject Categories

Catalysis and Reaction Engineering | Chemical Engineering | Transport Phenomena

Synthesis of Copper Oxide Nanoparticles in Droplet Flow Reactors

Christopher Reilly
Department of Chemical Engineering
University of New Hampshire
Durham, NH 03824

Abstract

Synthesis of metal oxide nanoparticles within droplet flow reactors is advantageous over batch synthesis due to the elimination of concentration and temperature gradients inside the reactor and prevention of reactor fouling. We present results on the synthesis of copper oxide nanoparticles using aqueous droplets of copper acetate and acetic acid inside a bulk stream of sodium hydroxide in 1-octanol. Varying the copper acetate, acetic acid, and sodium hydroxide concentration resulted in needle-like and plate-like nanoparticles of varying sizes. The rate of mass transfer from the bulk to the droplet phase was found to increase with flow rate and addition of surfactants.

1. Introduction

Copper oxide nanoparticles have unique optical and semiconductor properties allowing the application of copper oxide nanoparticles in many industrial applications[1]. Controlling the size and morphology of the nanoparticles enables tunability of these properties[2]. The major methods of synthesizing copper oxide nanoparticles involve one phase in either a batch or continuous flow reactor. Droplet flow reactors, where reagents are separated into different phases, offer several advantages over batch and single phase flow reactors. The droplets contain the synthesis reaction preventing reactor fouling[3], reducing concentration gradients[4,5], and increasing heat transfer[6]. However, droplets may merge within the droplet flow reactor, resulting in a sudden volume and interfacial area change. Uncontrolled droplet merging will affect the mass transfer from the bulk phase to the droplet phase and give inconsistent results. Surfactants can be added to the droplet phase to prevent any droplet merging, but may change the rate of mass transfer and create concentration and surface tension gradients.

In this work, copper oxide nanoparticles were synthesized in a droplet flow reactor with aqueous droplets of copper acetate and acetic acid inside a bulk stream of sodium hydroxide in 1-octanol. The effect of reagent concentrations on the size and morphology of the nanoparticles as well as the effect of surfactant concentration on the mass transfer from the bulk to droplet phase were investigated.

2. Materials and Methods

2.1 Reagents

Copper (II) acetate monohydrate (ACS Grade, Acros Organics), glacial acetic acid (ACS Grade, Fisher Scientific), sodium hydroxide (ACS Grade, Fisher Scientific), 1-octanol (99% pure, Acros Organics), 190 proof ethanol (ACS Grade, Pharmco-Aaper), hydrochloric acid (ACS Grade, VWR Scientific), methyl orange (ACS Grade, Acros Organics), and Triton X-100 (Alfa Aesar) were all used as received without further purification.

2.2 Solution Preparation

The required masses of copper acetate and acetic acid were dissolved in 100 mL of ultra-pure water (Milli-Q, 18.2 MΩ.cm) at room temperature. The required mass of sodium hydroxide was dissolved in 100 mL of 1-octanol. The sodium hydroxide solution was agitated, with a magnetic stir bar, for 24 hours at room temperature to fully dissolve the sodium hydroxide pellets. The required masses of hydrochloric acid and Triton X-100 (if required) were dissolved in 100 mL of ultra-pure water at room temperature. The required mass of methyl orange was dissolved in 100 mL of ultra-pure water at room temperature.

2.3 Flow Synthesis of Copper Oxide Nanoparticles

The reactor used for the two-phase flow synthesis of copper oxide nanoparticles comprised of four parts as shown in Figure 1. First, a co-flow drop formation apparatus was used to form droplets of aqueous copper acetate with acetic acid solution in pure 1-octanol. The inset shows an image of a droplet of copper acetate with acetic acid forming at the nozzle. Aqueous copper

acetate with acetic acid was pumped by a syringe pump, at a flow rate of 0.015 mL/min through

a 27 gauge stainless steel needle. The needle was concentrically placed in a cylindrical

polydimethylsiloxane (PDMS) channel, ID = 800 μm, that contained the flow of pure 1-octanol

at 0.075 mL/min. The stream of droplets exited the drop formation setup through a PTFE tube,

ID = 812 μm. Second, a stream of sodium hydroxide dissolved in 1-octanol was introduced to the

droplet stream using a T-junction. The sodium hydroxide in 1-octanol solution was pumped by a

syringe pump at a flow rate of 0.075 mL/min. Third, the PTFE tubing containing the droplet

reactors continued into a water bath at 60°C where copper oxide nanoparticles were synthesized

using a residence time of ten minutes. Fourth, the product from the reactor was collected in an

ice chilled round bottom flask containing 50 mL of 190 proof ethanol. For each trial, the product

from the reactor was collected for 30 minutes in the flask before preparing the product for

analysis.
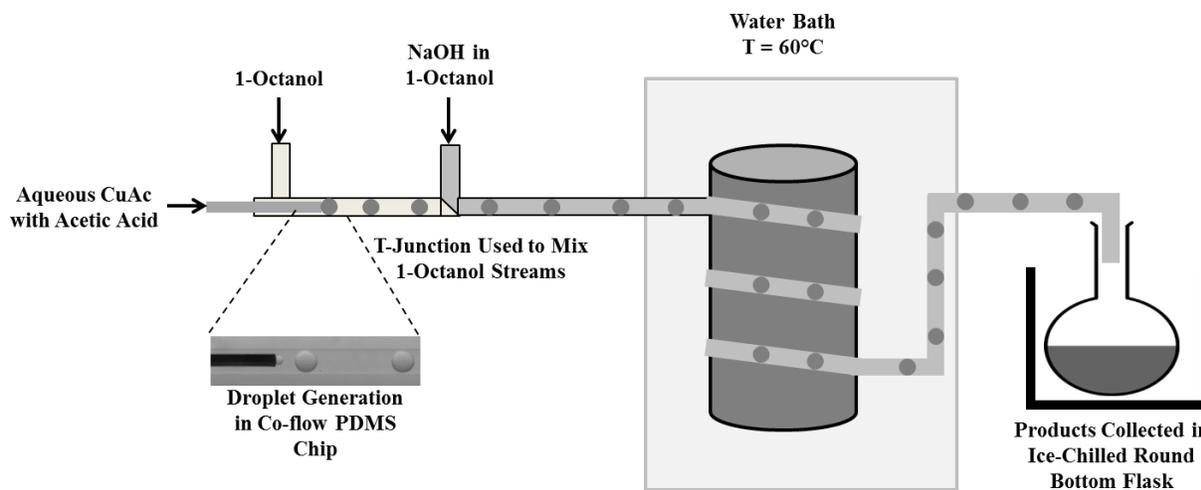
Figure 1. Schematic of the experimental setup for the synthesis of copper oxide nanoparticles in

a droplet flow reactor.

2.4 Nanoparticle Washing

After collecting the product for thirty minutes, the flask contents were split into four 50 mL centrifuge tubes and centrifuged at 4,000 rpm for 20 minutes in an Eppendorf 5702 Centrifuge. The supernatant was decanted until about 1 mL remained. The copper oxide nanoparticles were then dispersed into the remaining liquid and centrifuged at 13,000 rpm for 10 minutes in an Eppendorf Minispin Plus Centrifuge. The supernatant was decanted and replaced with fresh ethanol. The copper oxide nanoparticles were then dispersed into the ethanol using an ultrasonic bath. The centrifugation and washing steps were repeated four times. After the last centrifugation, the supernatant was decanted and the tubes were placed in a 60°C oven to evaporate any remaining liquid.

2.5 Size and Morphology Analysis

Images of the copper oxide nanoparticles were taken using a Tescan Lyra3 scanning electron microscope (SEM) using the in-beam secondary electron detector at an accelerating voltage of 6.0 kV. The copper oxide samples used in the SEM were first dispersed in acetone using an ultrasonic bath and then deposited on silicon wafer squares. Before viewing the SEM, the samples were sputter-coated with a gold-palladium layer to improve conductivity. Size measurements from the resulting images were made on manually selected nanoparticles until a sample size of 100 particles was achieved.

2.6 Energy Dispersive Spectroscopy (EDS)

Elemental analysis was conducted using an EDAX EDS system on the Lyra3 SEM with an acceleration of 20 kV and a magnification of 5400X.

2.7 X-Ray Diffraction (XRD)

X-ray diffraction of the nanoparticle samples was conducted on a Bruker-AXS diffractometer

with a general area detector diffraction system. The diffractometer was equipped with a copper

X-ray tube and CuKα 1 X-rays were used for the analysis, $\lambda = 1.54056$ Å.

2.8 Mass Transfer Analysis

The reactor used for the two-phase flow titration reaction to analyze mass transfer between the

phases comprised of three parts as shown in Figure 2. First, the same co-flow drop formation

apparatus as used in the flow synthesis of copper oxide nanoparticles was used to form droplets

of 0.087 M aqueous hydrochloric acid with methyl orange indicator and, if required, between

0.02 and 0.2 mM Triton X-100 solution in pure 1-octanol. Aqueous hydrochloric acid with

methyl orange was pumped by a syringe pump, at a flow rate between 0.015 and 0.030 mL/min

through a 27 gauge stainless steel needle. The needle was concentrically placed in a cylindrical

polydimethylsiloxane (PDMS) channel, ID = 800 μm that contained the flow of pure 1-octanol at

flow rates between 0.075 and 0.150 mL/min. The stream of droplets exited the drop formation

setup through a PTFE tube, ID = 812 μm. Second, a stream of 0.1 M sodium hydroxide in 1-

octanol solution was introduced to the droplet stream using a T-junction. The sodium hydroxide

in 1-octanol was pumped by a syringe pump at a flow rate between 0.075 and 0.150 mL/min.

Third, the rate of mass transfer of sodium hydroxide into the droplet phase within the PTFE tube

was measured by observing the length of the PTFE tube required to achieve the color change of

orange to yellow/clear in the droplet. Once the color change was observed and the hydrochloric

acid was neutralized, the reagents were collected in a waste container.
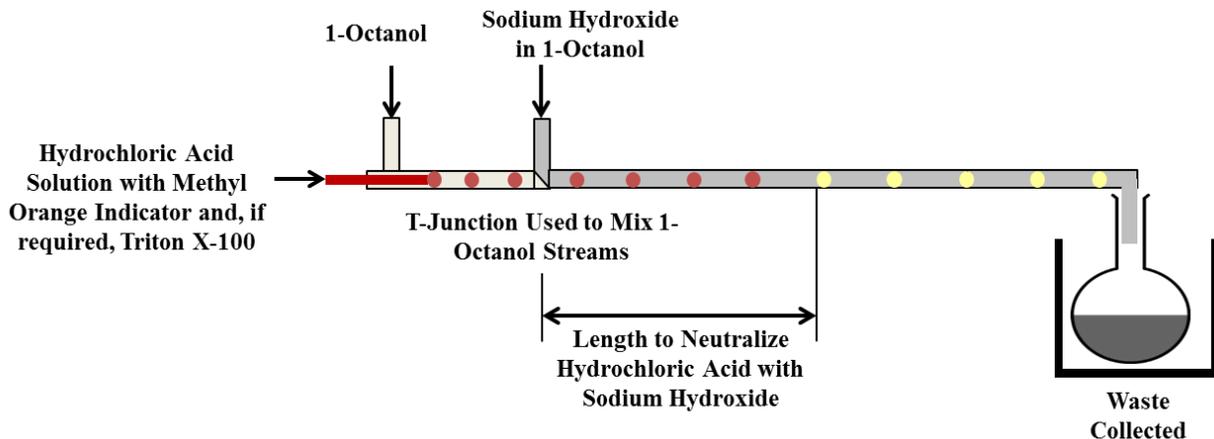
Figure 2. Schematic of the experimental setup for the mass transfer analysis in a droplet flow reactor.

3. Results and Discussion

The continuous synthesis of copper oxide nanoparticles was achieved using a co-flow droplet phase reactor. The nanoparticles were washed and dried for the analysis of the composition, size, and shape. The XRD and EDS analysis of the copper oxide nanoparticles confirm that copper (II) oxide was synthesized in the reactor (Figure 3). The two peaks of the XRD analysis at (-111) and (111) align with the peaks of copper (II) oxide and not with copper (I) oxide. Although the sample for the XRD analysis was limited and resulted in only two peaks, the peaks align solely with copper (II) oxide and it is very likely the product is in fact copper (II) oxide. A larger sample for the XRD analysis would confirm this result. The EDS shows major peaks of copper and oxygen at a one-to-one ratio. The largest peak corresponds to the silicon substrate on which the sample was deposited. The one-to-one ratio of copper to oxygen further confirms that the product is copper (II) oxide and not copper (I) oxide.

(a)

(b)

Element	Atomic %	Error %
O K	51.64	10.19
Cu K	48.36	3.67
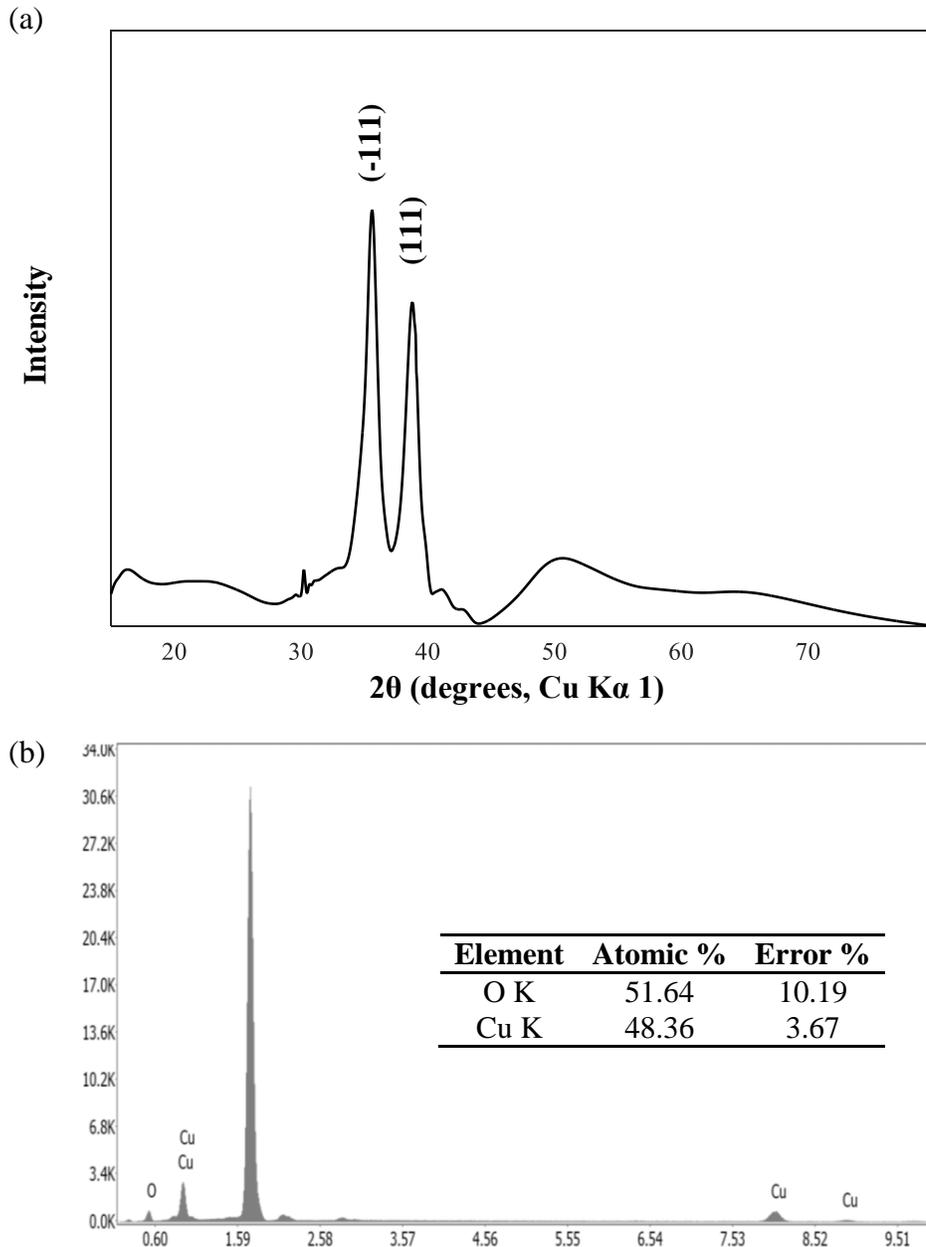
**Figure 3.** (a) XRD and (b) EDS results for the copper oxide nanoparticles synthesized.

3.1 The Effect of Copper Acetate Concentration

The concentration of the copper acetate solution in the droplet phase was changed from 0.01 M

to 0.02 M at a reaction temperature of 60°C, hydroxide concentration of 0.1 M, residence time of

10 minutes, and a total flow rate of 0.165 mL/min. The SEM images in Figure 4 show the

8

needle-like nanoparticles. The length and width of 100 particles were measured for each image. Table 1 shows the average length and width of the particles for the two different concentrations of copper acetate. Increasing the copper acetate concentration in the droplet phase resulted in an increased length and width of the needle-like particles. As more copper acetate is present, the particles can grow larger, both in length and in width. The trend of increased particle length and diameter with increased copper acetate concentration is expected to hold until a maximum occurs with the limited sodium hydroxide able to diffuse into the droplet.
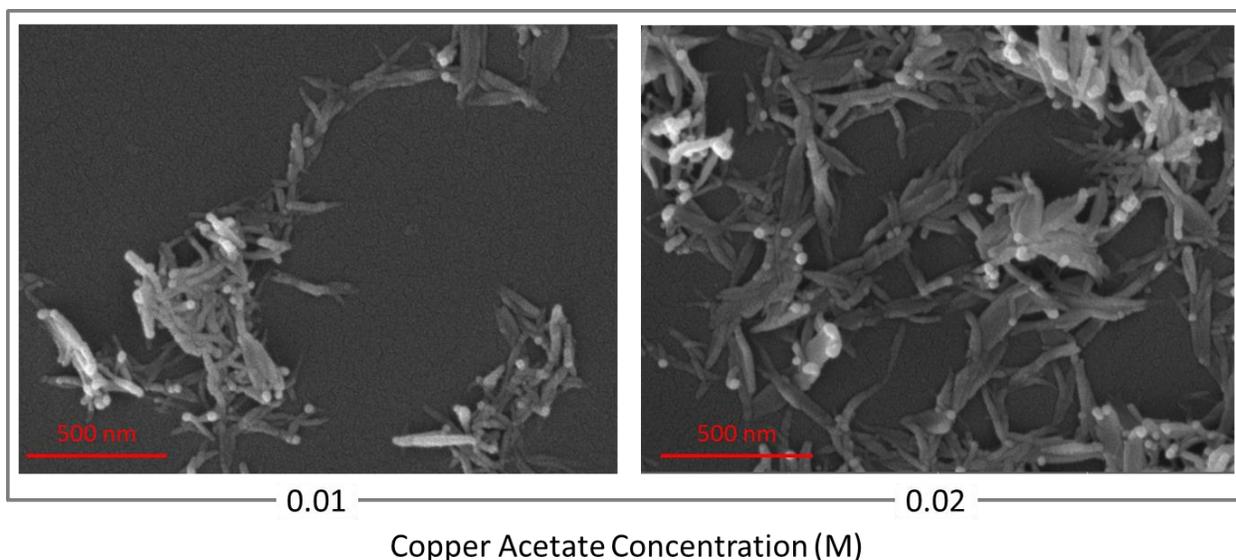
Figure 4. SEM micrographs showing the effect of copper acetate concentration on nanoparticle size.
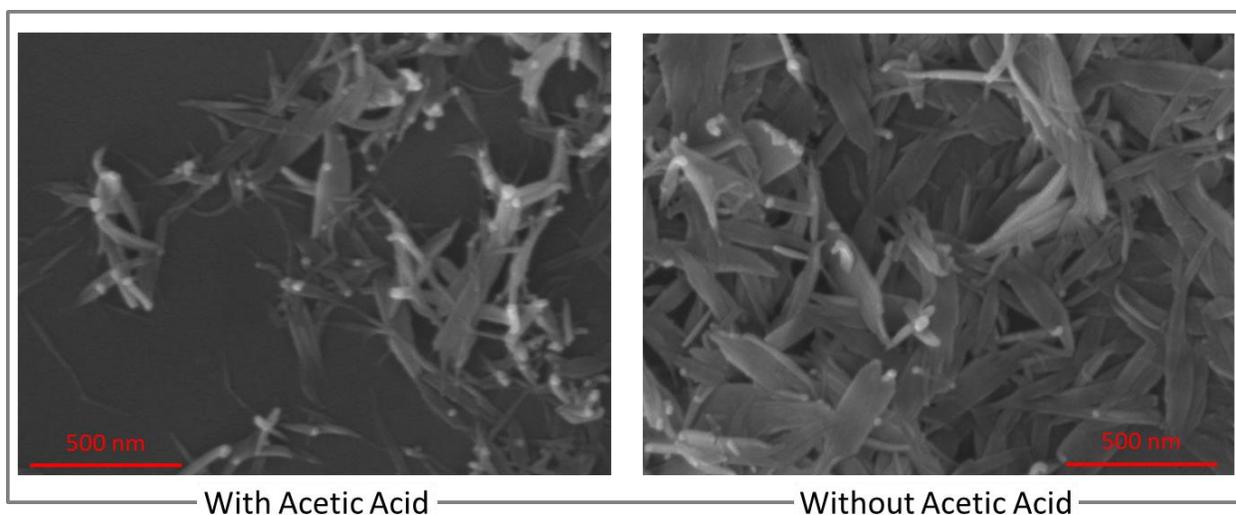
Table 1. Average values of particle length and width for nanoparticles synthesized with different concentrations of copper acetate for 100 particles.

$[Cu^{2+}]$ (M)	Length (nm)	Width (nm)
0.01	177	26.2
0.02	233	35.7

3.2 Effect of Sodium Hydroxide Concentration

The concentration of the sodium hydroxide in the bulk phase was changed from 0.05 M to 0.1 M at a reaction temperature of 60°C, copper acetate concentration of 0.01 M, residence time of 10 minutes, and a total flow rate of 0.165 mL/min. The SEM images in Figure 5 show the resulting sizes and shapes of the nanoparticles. The lower sodium hydroxide concentration resulted in varied particle size and shape. Plate-like particles, needle-like particles, as well as some spherical particles of many different sizes were seen at the lower sodium hydroxide concentration. The higher sodium hydroxide concentration yielded a more uniform particle size and morphology of needle-like particles. The SEM images did not show enough particles to get an accurate measure of the average size of the nanoparticles. The non-uniform particle size and morphology at the lower hydroxide concentration may be due to inconsistent diffusion of the hydroxide into the droplet at such low concentrations. The small range of sodium hydroxide concentration tested does not allow for full analysis of the effect on particle size and morphology, but it appears that increased hydroxide concentration results in needle-like particles with more uniform size.

Figure 5. SEM micrographs showing the effect of sodium hydroxide concentration on nanoparticle size and shape.

3.3 Effect of Acetic Acid Concentration

The effect of the presence of acetic acid in the droplet phase on the size and morphology of the nanoparticles was analyzed. It was reported that acetic acid would prevent the hydrolysis of the copper acetate solution in a batch reactor[7]. Figure 6 shows the SEM images of the copper oxide nanoparticles with and without acetic acid present. Without any acetic acid present, the nanoparticles become plate-like and have a variety of sizes. The copper oxide nanoparticles have a more narrow size distribution and are needle-like when the acetic acid is present. The SEM images did not show enough particles to get an accurate measure of the average size of the nanoparticles, but the result can be clearly seen in the images. As expected from reports of batch synthesis of copper oxide nanoparticles, synthesis without acetic acid results in uncontrolled particle shapes and sizes.

Figure 6. SEM micrographs showing the effect of the presence of acetic acid in the droplet phase on the nanoparticle size and shape.

After understanding the effects of the reagent concentrations, the effect of surfactants within the droplet phase could be analyzed. The surfactant addition to the droplet phase would prevent any droplet merging within the reactor. If droplet merging occurs at any point in the reactor, the mass transfer from the bulk to the droplet will change due to a change in the interfacial area. This mass transfer change will have uncontrolled effects on the nanoparticle size and morphology. Although the surfactant addition will aid in controlling the size and shape of the nanoparticles synthesized, it may have adverse effects as well. Since the surfactants would align on the interface of the droplet, the surfactants may add a layer of mass transfer resistance and limit the mass transfer from the bulk to the droplet phase. The surfactants may also create concentration and surface tension gradients as the surfactants are dragged via viscous forces on the moving droplet. These gradients may cause enhanced convection and can affect the rate of mass transfer from the bulk to the droplet phase. The surfactants may also serve as a nucleation site for the

nanoparticles and affect the growth of the particles. It will be necessary to analyze the effects of surfactants on mass transfer and on particle nucleation and growth separately.

3.4 Effect of Flow Rate on Mass Transfer

Prior to analyzing the effect of surfactant concentration on mass transfer, the rate of mass transfer from the bulk to the droplet phase must be analyzed. This rate of mass transfer can be analyzed using a titration reaction with the setup shown in Figure 2. As the sodium hydroxide in the bulk phase diffuses into the droplet phase, it reacts with hydrochloric acid present in the droplet phase and neutralizes the droplet. An indicator present in the droplet changes color when the droplet is neutralized. The location within the reactor that the neutralization is observed to occur corresponds to a time that it takes to neutralize the droplet. The time taken to neutralize the droplet is inversely proportional to the rate of mass transfer from the bulk phase to the droplet phase.

The total flow rate within the reactor was changed from 0.165 mL/min to 0.330 mL/min while keeping the ratio of the droplet to bulk flow rates constant, and the concentrations of the reagents constant. Figure 7 shows the effect of the flow rate on the time taken to neutralize the droplet. The triangular and circular data points represent trials that were conducted on different days. Although the overall trend appears to peak around 0.220 mL/min, the trials conducted on the same day show the same trend of decreased time to neutralize with increased flow rate. It is expected that if all trials were conducted on the same day, a linear trend of decreased time to neutralize with increased flow rate would result. The variation between days is likely due to fluctuations in room temperature and reagents coming out of solution. As the flow rate of the

reactor increases, the convection increases and the rate of mass transfer increases resulting in a decreased time to neutralize the droplet.
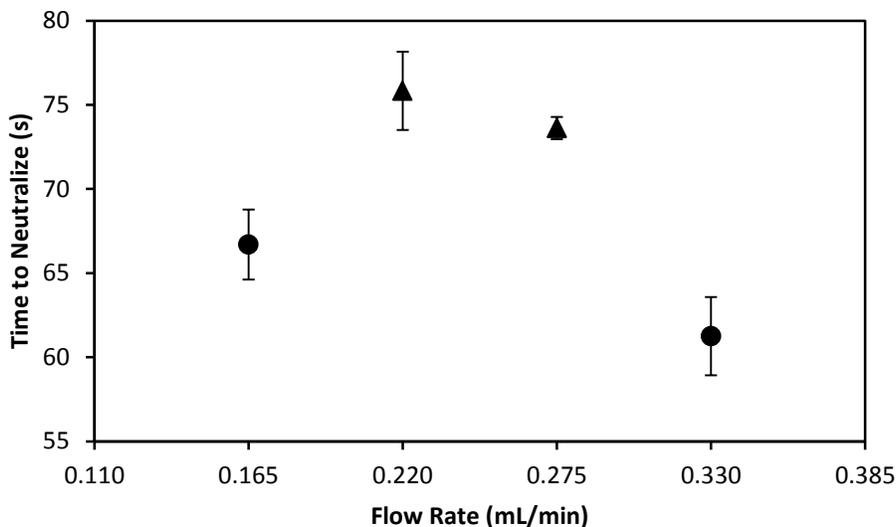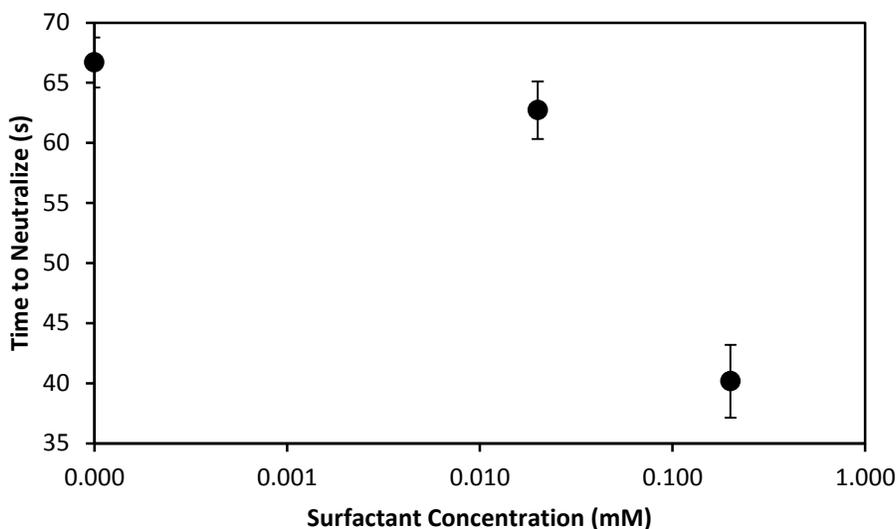

Figure 7. Average time taken to neutralize the droplet within the droplet flow reactor at various flow rates.

3.5 Effect of Surfactant Concentration on Mass Transfer

Surfactants were added to the droplet phase of the mass transfer experimental setup at concentrations from 0.02 mM to 0.2 mM at a total flow rate of 0.165 mL/min and constant reagent concentrations. As seen in Figure 8, the time taken to neutralize the droplet decreases with increased surfactant concentration. It was expected that the added layer of mass transfer resistance of the surfactant on the droplet interface would have more of an effect than the increased convection due to additional concentration and surface tension gradients in the reactor. Increasing the surfactant concentration was expected to increase the time to neutralize and therefore decrease the rate of mass transfer from the bulk to the droplet phase. It was observed, however, that the rate of mass transfer increased with increased surfactant concentration. The

surfactants created surface tension and concentration gradients along the interface of the droplet that increased convection and increased the rate of mass transfer.

Figure 8. Average time taken to neutralize the droplet within the droplet flow reactor at various surfactant concentrations.

4. Conclusions

Copper oxide nanoparticles were successfully synthesized using a two-phase reactor with aqueous copper acetate and acetic acid droplets and a 1-octanol bulk phase containing sodium hydroxide. The size and shape of the copper oxide nanoparticles were found to be controlled by controlling the reagent concentrations. Increased copper acetate concentration increased particle length and width, increased sodium hydroxide concentration resulted in more uniform particle size and morphology, and the presence of acetic acid resulted in needle-like particles with a narrow size distribution. Greater ranges of each parameter studied would be beneficial to understand further how to control the size and shape of the copper oxide nanoparticles. The

effect of surfactant addition on the synthesis of the nanoparticles was also of interest, requiring the determination of the effect of flow rate and surfactant concentration on the rate of mass transfer. The rate of mass transfer from the bulk phase to the droplet phase was found to increase with flow rate as well as increase with surfactant concentration. The effect of surfactant concentration on the nanoparticle nucleation and growth can be analyzed. These results would ultimately allow for the analysis of the effect of surfactant concentration on the size and morphology of the copper oxide nanoparticles.

Acknowledgements

References

(1) Y. Bai, T. Yang, Q. Gu, G. Cheng and R. Zheng, "Shape control mechanism of cuprous oxide nanoparticles in aqueous colloidal solutions", Powder Technology, vol. 227, pp. 35-42, 2012.

(2) T. Nguyen, "From formation mechanisms to synthetic methods toward shape-controlled oxide nanoparticles", Nanoscale, vol. 5, no. 20, p. 9455, 2013.

(3) A. Nightingale and J. deMello, "Microfluidics: Segmented Flow Reactors for Nanocrystal Synthesis (Adv. Mater. 13/2013)", Advanced Materials, vol. 25, no. 13, pp. 1806-1806, 2013.

(4) J. Tice, H. Song, A. Lyon and R. Ismagilov, "Formation of Droplets and Mixing in Multiphase Microfluidics at Low Values of the Reynolds and the Capillary Numbers", Langmuir, vol. 19, no. 22, pp. 9127-9133, 2003.

(5) S. Teh, R. Lin, L. Hung and A. Lee, "Droplet microfluidics", Lab on a Chip, vol. 8, no. 2, p. 198, 2008.

(6) P. Urbant, A. Leshansky and Y. Halupovich, "On the forced convective heat transport in a droplet-laden flow in microchannels", Microfluidics and Nanofluidics, vol. 4, no. 6, pp. 533-542, 2007.

(7) J. Zhu, D. Li, H. Chen, X. Yang, L. Lu and X. Wang, "Highly dispersed CuO nanoparticles prepared by a novel quick-precipitation method", Materials Letters, vol. 58, no. 26, pp. 3324-3327, 2004.